Penerbit Akademia Baru

Journal of Advanced Research in Experimental Fluid Mechanics and Heat Transfer

http://www.akademiabaru.com/submit/index.php/arefmht
ISSN: 2756-8202

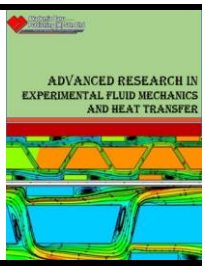

Solute Dispersion in Casson Blood Flow through a Stenosed Artery with the Effect of Temperature and Electric Field

Nur Husna Amierah Mohd Zaperi[1], Nurul Aini Jaafar[1,*], Duraisamy Sambasivam Sankar[2]

[1] Department of Mathematical Sciences, Faculty of Science, Universiti Teknologi Malaysia, 81310 Johor Bahru, Johor, Malaysia
[2] School of Applied Sciences and Mathematics, University Teknologi Brunei, Jalan Tunku Link Gadong BE, 1410 Brunei Darussalam

ABSTRACT

This study develops a mathematical model to address solute dispersion in arterial blood flow, particularly considering the effects of temperature and electric fields using the Casson fluid model. Given the physiological importance of drug delivery within the human vascular system, understanding these dynamics is crucial, especially in the presence of cardiovascular diseases (CVD). The Generalized Dispersion Model (GDM) is employed to simulate the dispersion function. Results demonstrate that elevated temperatures and electric fields enhance drug uptake and distribution by increasing blood flow. The model accurately predicts drug behavior in narrowed arteries, optimizing dosage regimens and improving therapeutic outcomes. Visual representations and detailed discussions of these findings are presented in the subsequent sections. The results are validated against a previous study that did not consider the effects of stenosis height, temperature and electric field. The findings suggest a strong agreement between the two studies. Additionally, an increase in mean absorption leads to an increase in velocity. When mean absorption increases, the functions of steady dispersion and overall dispersion decrease, while the function of unsteady dispersion increases. The reverse behavior is observed for the electric field. The study concludes that integrating temperature and electric field effects into drug delivery systems can significantly enhance treatment efficacy and reduce side effects, providing a valuable tool for advanced targeted therapies in CVD and cancer management.

Keywords:
Blood flow; Casson fluid; electric field; Generalized Dispersion Model; solute dispersion; temperature

Received: 15 June 2024 | **Revised: 25 August 2024** | **Accepted: 30 August 2024** | **Published: 15 September 2024**

1. Introduction

The circulatory system, comprising the heart, blood vessels, and blood, is fundamental in maintaining the body's homeostasis by ensuring the continuous flow of blood, which delivers oxygen and nutrients to tissues while removing waste products is taken from [1]. However, the presence of stenosis, or the narrowing of blood vessels, can significantly impede this flow. Stenosis often results from the buildup of plaque in the arteries, a condition known as atherosclerosis is taken from [2]. This reduced blood flow can lead to CVD, such as coronary artery disease, heart attacks, and strokes is taken from [3]. Additionally, chronic cardiovascular conditions may create an environment that promotes cancer development. For instance, the hypoxic (low oxygen) conditions due to impaired

* *Corresponding author.*
E-mail address: nurulaini.jaafar@utm.my

https://doi.org/10.37934/arefmht.17.1.1434

blood flow can contribute to tumor growth and metastasis. The interplay between CVD and cancer underscores the complexity of these diseases and highlights the importance of maintaining vascular health to prevent a cascade of adverse health outcomes.

Temperature is one of the effects that causes the development of cancer. The relationship between temperature, blood flow, and cancer is intricate and impactful. The body maintains its core temperature around 37°C (98.6°F) through mechanisms such as vasodilation and vasoconstriction, which regulate blood flow to either dissipate or retain heat is taken from [4]. Blood flow regulates body temperature, distributing heat throughout the body via circulation, which in turn affects cellular metabolism and overall physiological functions is taken from [5]. In cancer, abnormal blood vessel formation and altered flow patterns can cause localized temperature variations within tumors, known as tumor thermal heterogeneity, influencing diagnosis and treatment monitoring using thermal imaging and thermography. Furthermore, blood flow is crucial for drug delivery in cancer therapy, where adequate perfusion is essential for transporting therapeutic agents to tumor sites. Challenges arise from irregular blood flow, limiting drug penetration and efficacy, prompting research into strategies like enhancing vascular perfusion or employing hyperthermia to optimize drug uptake and treatment outcomes. Understanding these interdependencies is critical for advancing targeted therapies and improving cancer management strategies.

Besides, the relationship between electric fields and cancer involves various mechanisms, including their potential use in drug delivery and their influence on blood flow. Electric fields can be applied externally or internally to modulate cellular functions, such as enhancing drug uptake into cancer cells through electroporation or triggering apoptosis. In drug delivery, electric fields can help nanoparticles or drugs traverse cellular barriers more efficiently, targeting specific cancerous tissues while minimizing systemic side effects. Additionally, electric fields can affect blood flow by influencing vascular permeability and altering blood vessel functions, potentially impacting tumor growth and metastasis. The interaction between electric field and blood's biological components has the potential to be critical from a variety of perspectives, including understanding the biophysics under sick situations and rapid illness diagnoses is taken from [6]. Research into the therapeutic and physiological effects of electric fields continues to explore their role in cancer treatment strategies and their interaction with the circulatory system to improve therapeutic outcomes.

This research is differed in that it models solute dispersion within blood flow through stenosed arteries by combining influences of temperature and electric field. Temperature and electric fields significantly impact drug delivery, particularly in the context of CVD and blood flow dynamics. Elevated temperatures can increase blood flow and vessel permeability, enhancing drug dispersion and uptake by tissues. Electric fields, similarly, can facilitate targeted drug delivery by altering cell membrane permeability and aiding in the precise placement of therapeutic agents. In the presence of CVD, the behavior of blood, often modeled as a Casson fluid, changes due to altered viscosity and shear rates in narrowed or obstructed arteries. These changes affect the way drugs are dispersed and interact with the vascular walls. Shear rates, which describe the deformation of blood flow, are particularly important in CVD, as they influence the adhesion of drugs to vessel walls and their subsequent absorption. Understanding the interplay between temperature and electric fields in blood flow is crucial in medical research and bioengineering for optimizing drug delivery systems, ensuring effective treatment, and minimizing side effects in patients with cardiovascular conditions.

A non-Newtonian fluid with yield stress, such as the Casson fluid model, is valuable for simulating blood flow in narrow arteries. The Casson fluid model is particularly effective due to its shear-thinning behavior at infinite shear rates, infinite yield stress, and zero viscosity. Blair [7] demonstrated that blood's fundamental shear behavior in small arteries aligns well with the Casson fluid model. Casson [8] further assessed this model's suitability, finding that blood exhibits a nonzero yield stress at low

shear rates. According to Merrill *et al.,* [9], the Casson fluid model accurately predicts blood flow characteristics in tubes with varying diameters of $130 - 1000\mu m$. Murugan *et al.,* [10] analyzed the unsteady dispersion of solute in pulsatile flow of electro-magneto-hydrodynamic fluid in a tube packed with a porous medium using the Casson fluid model. An unsteady convective-diffusion equation was applied in their study. Noranuar *et al.,* [11] investigated the analytical simulation of magnetohydrodynamic Casson blood flow with CNTs in a channel under atherosclerotic conditions. Azmi *et al.,* [12] analyzed the effects of porosity and slip velocity on MHD pulsatile Casson fluid flow in a cylinder.

Understanding drug delivery is crucial for developing effective treatments, minimizing side effects, and ensuring that therapeutic agents reach their intended targets within the body. This is especially important for treating illnesses like cancer, when it's crucial to precisely target chemotherapy medications to the tumor cells in order to maximize treatment effectiveness and reduce harm to healthy organs. Obstacles like the blood-brain barrier, which restricts medication distribution to the brain, highlight the need for creative delivery techniques that can get beyond biological barriers and distribute therapeutic agents to the precise locations where they are most required. Improving patient outcomes like side effects and reducing pain for a variety of diseases and developing new medical treatments depend on addressing these issues through sophisticated mathematical modeling and customized medication delivery technology. Mathematical modeling plays a pivotal role in this process by applying the GDM and the convective diffusion equation to predict drug dispersion and interactions within tissues.

The GDM accounts for the spread of drug particles considering molecular diffusion and blood flow, while the convective diffusion equation describes drug transport due to diffusion and blood convection. These models are particularly relevant in CVD, where blood behaves as a Casson fluid with altered viscosity and shear rates in narrowed arteries, affecting drug dispersion and absorption. By simulating various physiological conditions, mathematical models help optimize dosage regimens, improve drug targeting, and enhance therapeutic outcomes. This predictive capability is vital for refining drug delivery systems to ensure medications effectively reach diseased tissues, thereby improving treatment efficacy and reducing adverse effects.

GDM plays a crucial role in describing the mechanisms of dispersion in microvascular blood flow. Early work by Taylor [13] and Aris [14] pioneered the understanding of solvent dispersion phenomena. Taylor [13] specifically examined solute dispersion in a straight tube with consistent laminar flow, considering variations in cross-sectional velocity and molecular diffusion. Concurrently, Gill and Sankarasubramanian [15] applied the moment approach to quantify effective dispersion coefficients under pulsatile flow conditions. They later proposed the GDM is taken from [16] to study solute dispersion, exploring factors like exchange, convection, and scattering in the presence of wall reactions. Zaperi and Jaafar [17] examined dispersion of solute in blood flow under the influence of an electric field through an artery, employing the Casson fluid model in conjunction with the GDM. Zaperi and Jaafar [18] also analyzed the dispersion of solute in blood flow under the influence of a magnetic field through a stenosed artery, using the Casson fluid model in conjunction with the GDM.

The literature review highlights the limited research on the dispersion of solutes in arterial blood flow, particularly regarding the effects of temperature and electric fields using the Casson fluid model. This gap is critical due to its physiological importance for drug delivery within the human vascular system. Consequently, this study aims to develop a mathematical model for the dispersion of solutes in arterial blood flow, incorporating the effects of temperature and electric fields. The research employs the Casson fluid model in conjunction with the GDM to address this gap. In order to improve patient medical treatment and advance biomedical engineering, mathematical modeling is essential for interpreting the complex dynamics of blood flow in artery stenosis. This study aims to

address a critical gap in existing models, which frequently oversimplify or ignore the complex interactions between temperature and electric fields. This study aims to provide new computational methodologies in biomedical research and to improve the understanding of physiological fluid dynamics among academics by providing new mathematical insights into these processes. The following sections present visual representations of the findings and related discussions.

2. Methodology

2.1 Mathematical Formulation

The blood flow is measured using the system of polar cylindrical coordinates $(\bar{r}, \bar{\psi}, \bar{z})$, where the radial and axial coordinates designated by $\bar{r}$ and $\bar{z}$ respectively and the azimuthal angle denoted by $\bar{\psi}$. Figure 1 shows the geometry of pipe flow with the influence of electric field for Casson fluid model where $\bar{E}_z$ is electric field, $\bar{u}$ is the velocity of fluid flow, $\bar{\delta}$ is height of stenosis, $\bar{r}_p$ is the radius of the plug region in circular pipe, R_0 is the radius of artery and $\bar{L}$ is the length of conduit.

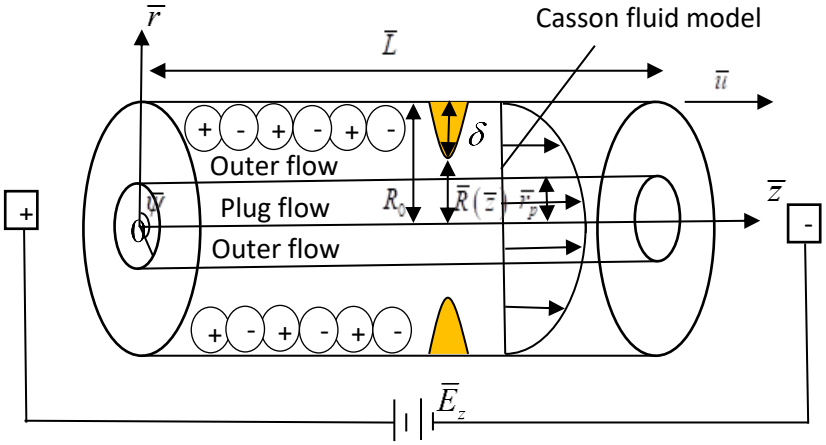

Fig. 1. The geometry of pipe flow with the influence of electric field for Casson fluid model

2.2 Governing Equations

The improved model incorporates complex multiphysics interactions brought about by applied temperature and electric fields in addition to fluid dynamics. By examining the way of temperature and electric fields alter blood flow behavior within stenosed arteries, this novel approach goes beyond traditional fluid mechanics investigations. Thus, the momentum equation with temperature and electric field for steady flow by Tiwari *et al.,* [19] is given as follows

$$\frac{\bar{\rho}\bar{\mu}}{r}\frac{d}{d\bar{r}}(\bar{r}\bar{\tau}) + \bar{g}\bar{\rho}\bar{\gamma}(\bar{T} - \bar{T}_\infty) - \sigma\bar{\rho}\rho_e\bar{E}_z - \frac{d\bar{p}^*}{d\bar{z}} = 0, \tag{1}$$

where $\bar{p}^*, \bar{\rho}, \bar{\mu}, \bar{g}, \bar{\gamma}, \bar{T}, \bar{T}_\infty, \sigma, \rho_e$ and $\bar{E}_z$ represent the fluid pressure, fluid density, temperature-dependent viscosity, acceleration due to gravity, absorption ratio, temperature, equilibrium temperature, electrical conductivity, and fluid density in an electric field and electric field, respectively. The boundary condition for momentum equation in Eq. (1) is given as

$$\bar{\tau} = \text{finite at } \bar{r} = 0. \tag{2}$$

According to Tiwari *et al.,* [19], the following is the energy equation that affect the flow

$$\overline{K}\left(\frac{\partial^2\overline{T}}{\partial\overline{r}^2}+\frac{1}{\overline{r}}\frac{\partial\overline{T}}{\partial\overline{r}}\right)+\overline{Q}=0, \tag{3}$$

where $\overline{K}$ is the thermal conductivity and $\overline{Q}$ is the constant heat absorption. According to Tiwari *et al.,* [19], the boundary condition of temperature in Eq. (3) is given as follows

$$\frac{d\overline{T}}{d\overline{r}}=0 \text{ at } \overline{r}=\overline{R}(\overline{z}) \tag{4}$$

and

$$\overline{T}=\overline{T}_w \text{ at } \overline{r}=\overline{R}(\overline{z}). \tag{5}$$

In this study, new development in Casson blood flow mathematical modeling is presented by including more advanced temperature-dependent viscosity profiles in the constitutive of Casson fluid as defined as follows

$$-\frac{d\overline{u}}{d\overline{r}}=\begin{cases}\frac{1}{\overline{\mu}(\overline{T})}\left(\sqrt{\overline{\tau}}-\sqrt{\overline{\tau}_y}\right)^2 & \text{if } \overline{\tau}>\overline{\tau}_y,\\ 0 & \text{if } \overline{\tau}<\overline{\tau}_y,\end{cases} \tag{6}$$

where

$$\overline{\mu}(\overline{T})=\overline{\mu}e^{-\alpha\left(\frac{\overline{T}-\overline{T}_\infty}{\overline{T}_w-\overline{T}_\infty}\right)}, \tag{7}$$

where $\overline{\mu}, \alpha(\ll 1), \overline{\tau}_y, \overline{u}$ and $\overline{T}_w$ are the viscosity coefficient of Casson fluid model, viscosity parameter index, yield stress, axial velocity of the fluid flow, and temperature of vessel wall. According to Verma *et al.,* [20], the slip boundary condition of constitutive equation is given as

$$\overline{u}=\overline{u}_s \text{ at } \overline{R}(\overline{z}), \tag{8}$$

where

$$\overline{R}(\overline{z})=R_0\left(1-\frac{\overline{\delta}}{R_0}e^{\left(-\frac{\overline{k}^2\overline{\varepsilon}^2\overline{z}^2}{R_0^2}\right)}\right), \tag{9}$$

where $\overline{R}(\overline{z})$ is the radius of the stenosed segment, $\overline{\delta}$ is the height of stenosis at the middle point and $\overline{k}$ is the parametric constant and radius, $\overline{\varepsilon}=R_0/\overline{L}_0$. Consider the geometry of stenosis in Eq. (9) as follows

$$\frac{\overline{R}(\overline{z})}{R_0}=1-ae^{-bz^2}, \tag{10}$$

where $a=\overline{\delta}/R_0$ and $b=\overline{k}^2\overline{\varepsilon}^2/R_0^2$. Non-dimensional for Eq. (10) as below

$$R(z)=1-a_1e^{(-b_1z^2)}, \tag{11}$$

where $a_1 = \delta$ and $b_1 = bR_0^2$. The mean velocity is stated as follows

$$\bar{u}_m = \frac{2}{\bar{R}^2(z)}\left(\int_0^{\bar{r}_p} \bar{u}(\bar{r}_p)\bar{r}d\bar{r} + \int_{\bar{r}_p}^{\bar{R}(\bar{z})} \bar{u}(\bar{r})\bar{r}d\bar{r}\right). \tag{12}$$

The general of unsteady convective-diffusion equation in cylindrical coordinate systems is given by

$$\frac{\partial \bar{C}}{\partial \bar{t}} = -\bar{\mu}_z \frac{\partial \bar{C}}{\partial \bar{z}^*} + \bar{D}_m \left(\frac{1}{\bar{r}}\frac{\partial}{\partial \bar{r}}\left(\bar{r}\frac{\partial \bar{C}}{\partial \bar{r}}\right) + \frac{\partial^2 \bar{C}}{\partial \bar{z}^{*2}}\right), \tag{13}$$

where $\bar{C}$ is the concentration of the solute as a function of $\bar{r}$ (radial coordinate for circular pipe), $\bar{t}$ is the time, $\bar{u}_z$ is the velocity in $\bar{z}$ direction and $\bar{D}_m$ is the molecular diffusivity. Simplify Eq. (13), it yields

$$\frac{\partial \bar{C}}{\partial \bar{t}} + \bar{u}\frac{\partial \bar{C}}{\partial \bar{z}^*} = \bar{D}_m \left(\ell^2 + \frac{\partial^2}{\partial \bar{z}^{*2}}\right)\bar{C}, \tag{14}$$

where

$$\ell^2 = \frac{1}{\bar{r}}\frac{\partial}{\partial \bar{r}}\left(\bar{r}\frac{\partial}{\partial \bar{r}}\right). \tag{15}$$

The initial condition of convective diffusion coefficient is given by Gill and Sankarasubramanian [16]

$$\bar{C}(\bar{r}, \bar{z}, 0) = \begin{cases} C_0 \text{ if } |\bar{z}| \leq \frac{\bar{z}_s}{2}, \\ 0 \text{ if } |\bar{z}| > \frac{\bar{z}_s}{2}, \end{cases} \tag{16}$$

where C_0 is the concentration referenced and $\bar{z}_s$ is the length of solute. The boundary condition following Gill and Sankarasubramanian [16] is

$$\bar{C}(\bar{r}, \infty, \bar{t}) = 0, \tag{17}$$

the boundary condition of symmetry at the central circular pipe $\bar{r} = 0$ is

$$\frac{\partial \bar{C}}{\partial \bar{r}}(0, \bar{z}, \bar{t}) = 0 \tag{18}$$

and the boundary condition of the solute concentration gradient at the wall $\bar{r} = \bar{R}(\bar{z})$ is given by

$$\frac{\partial \bar{C}}{\partial \bar{r}}(\bar{R}(\bar{z}), \bar{z}, \bar{t}) = 0. \tag{19}$$

2.3 Non-Dimensional Variables

$$r = \frac{\bar{r}}{R_0}, \tau = \frac{\bar{\tau}R_0}{\bar{\mu}u_0}, p = \frac{\bar{p}\bar{\mu}u_0}{R_0}, z = \frac{\bar{z}}{R_0}, u = \frac{\bar{u}}{u_0}, \tau_y = \frac{\bar{\tau}_y R_0}{\bar{\mu}u_0}, u_s = \frac{\bar{u}_s}{u_0}, R(z) = \frac{\bar{R}(\bar{z})}{R_0}, r_p = \frac{\bar{r}_p}{R_0},$$
$$\gamma = \frac{\bar{Q}R_0^2}{\bar{K}(\bar{T}_w - \bar{T}_\infty)}, z_s = \frac{\bar{D}_m \bar{z}_s}{\bar{a}^2 u_0}, t = \frac{\bar{D}_m \bar{t}}{\bar{a}^2}, \theta = \frac{\bar{T} - \bar{T}_\infty}{\bar{T}_w - \bar{T}_\infty}, G_r = \frac{\bar{g}\bar{\rho}\gamma R_0^2(\bar{T}_w - \bar{T}_\infty)}{u_0\bar{\mu}}, C = \frac{\bar{C}}{C_0},$$

$$z^* = \frac{\bar{D}_m \bar{z}^*}{\bar{a}^2 u_0}, H = \frac{\bar{H}}{H_0}, \tag{20}$$

where $\tau, p, u_0, r, z^*, u, R_0, z, C, z_s, \tau_y, u_s, R(z), r_p, \gamma, \theta, t$ and G_r are shear stress, pressure gradient, fluid characteristic velocity, radial coordinate, radial direction for convective diffusion equation, velocity, the radius of artery in outer region, radial direction, concentration of solute, solute length, yield stress, slip velocity, stenosed radius respectively in non-dimensional variables, radius of artery in plug flow region, mean absorption coefficients, temperature in outer flow region, time and Grashof number.

2.4 Method of Solution

By using non-dimensional variables of Eq. (20) into Eq. (1), the momentum equation with temperature and electric field with respect to r is given as follows

$$\frac{A_1}{r}\frac{d}{dr}(r\tau) + G_r\theta + \sigma\rho\rho_e\varepsilon E_z + P = 0, \tag{21}$$

where $A_1 = \rho\mu^2 u_0 / R_0^2$. By substituting Eq. (20) into Eq. (3), non-dimensional of energy equation in Eq. (3) is given as follows

$$\frac{d^2\theta}{dr^2} + \frac{1}{r}\frac{d\theta}{dr} + \gamma = 0 \tag{22}$$

and by substituting Eq. (20) into Eq. (6), non-dimensional for constitutive equation of Casson fluid in Eq. (6) is given as follows

$$-\frac{du}{dr} = \tau + \tau_y - 2\sqrt{\tau}\sqrt{\tau_y}. \tag{23}$$

Substitute Eq. (20) into boundary conditions in Eq. (4) and (5). It shown as follows

$$\frac{d\theta}{dr} = 0 \text{ at } r = R(z) \tag{24}$$

and

$$\theta = 1 \text{ at } r = R(z). \tag{25}$$

Ordinary differential equation (ODE) in Eq. (22) is solved using linear differential equation. Apply Eq. (24) and (25) into Eq. (22). It is given as follows

$$\theta = \frac{\gamma r^2}{4} + 1 - \frac{\gamma R_z^2}{4}. \tag{26}$$

Substituting Eq. (26) into Eq. (21) is given as follows

$$\frac{A_1}{r}\frac{d}{dr}(r\tau) + G_r\left(\frac{\gamma r^2}{4} + 1 - \frac{\gamma R_z^2}{4}\right) + \sigma\rho\rho_e\varepsilon E_z + P = 0. \tag{27}$$

Integrating Eq. (27) with respect to r, it yields

$$\tau = -\frac{G_r\gamma r^3}{16A_1} - \frac{rG_r}{2A_1} + \frac{rG_r\gamma R_z^2}{8A_1} - \frac{\sigma\rho\rho_e\varepsilon E_z r}{2A_1} - \frac{rP}{2A_1} + C. \tag{28}$$

By substituting Eq. (20) into Eq. (2), the non-dimensional boundary condition of momentum equation yield

$$\tau = \text{finite at } r = 0. \tag{29}$$

Substituting Eq. (29) into Eq. (28), it yields

$$\tau = -\frac{G_r\gamma r^3}{16A_1} - \frac{rG_r}{2A_1} + \frac{rG_r\gamma R_z^2}{8A_1} - \frac{\sigma\rho\rho_e\varepsilon E_z r}{2A_1} - \frac{rP}{2A_1}. \tag{30}$$

Substituting $r = r_p$ and $\tau = \tau_y$ into Eq. (30). The expression for the yield stress is given as follows:

$$\tau_y = -\frac{G_r\gamma r_p^3}{16A_1} - \frac{r_pG_r}{2A_1} + \frac{r_pG_r\gamma R_z^2}{8A_1} - \frac{\sigma\rho\rho_e\varepsilon E_z r_p}{2A_1} - \frac{r_pP}{2A_1}. \tag{31}$$

Substituting Eq. (30) and (31) into Eq. (23), it forms

$$-\frac{du}{dr} = \left(-\frac{G_r\gamma r^3}{16A_1} - \frac{rG_r}{2A_1} + \frac{rG_r\gamma R_z^2}{8A_1} - \frac{\sigma\rho\rho_e\varepsilon E_z r}{2A_1} - \frac{rP}{2A_1}\right) + \left(-\frac{G_r\gamma r_p^3}{16A_1} - \frac{r_pG_r}{2A_1} + \frac{r_pG_r\gamma R_z^2}{8A_1} - \frac{\sigma\rho\rho_e\varepsilon E_z r_p}{2A_1} - \frac{r_pP}{2A_1}\right) - 2\sqrt{-\frac{G_r\gamma r^3}{16A_1} - \frac{rG_r}{2A_1} + \frac{rG_r\gamma R_z^2}{8A_1} - \frac{\sigma\rho\rho_e\varepsilon E_z r}{2A_1} - \frac{rP}{2A_1}}\sqrt{-\frac{G_r\gamma r_p^3}{16A_1} - \frac{r_pG_r}{2A_1} + \frac{r_pG_r\gamma R_z^2}{8A_1} - \frac{\sigma\rho\rho_e\varepsilon E_z r_p}{2A_1} - \frac{r_pP}{2A_1}}. \tag{32}$$

Simplify Eq. (32), it becomes

$$-\frac{du}{dr} = \left(\frac{r}{2} + \frac{r_p}{2}\right)\left(-\frac{G_r}{A_1} + \frac{G_r\gamma R_z^2}{4A_1} - \frac{\sigma\rho\rho_e\varepsilon E_z}{A_1} - \frac{P}{A_1}\right) + \left(\frac{r^3}{2} + \frac{r_p^3}{2}\right)\left(-\frac{G_r\gamma}{8A_1}\right) - 2\sqrt{\frac{r}{2}\left(-\frac{G_r}{A_1} + \frac{G_r\gamma R_z^2}{4A_1} - \frac{\sigma\rho\rho_e\varepsilon E_z}{A_1} - \frac{P}{A_1}\right) + \frac{r^3}{2}\left(-\frac{G_r\gamma}{8A_1}\right)}\sqrt{\frac{r_p}{2}\left(-\frac{G_r}{A_1} + \frac{G_r\gamma R_z^2}{4A_1} - \frac{\sigma\rho\rho_e\varepsilon E_z}{A_1} - \frac{P}{A_1}\right) + \frac{r_p^3}{2}\left(-\frac{G_r\gamma}{8A_1}\right)}. \tag{33}$$

Understanding the complexity of Casson models in explaining non-Newtonian blood flow via stenosed arteries and the influence of temperature and electric fields, this work employs the binomial expansion technique. The Casson equation's complex nonlinear terms can be approximated with this method, which improves computational feasibility and speeds up integration without compromising accuracy. Thus, applying binomial equation in Eq. (33) and integrate Eq. (33) with respect to r, it forms

$$u(r) = \frac{Ar^2}{4} + \frac{Br^4}{8} + \frac{Arr_p}{2} + \frac{Brr_p^3}{2} - \frac{2r\sqrt{Ar}\sqrt{r_p\left(A + Br_p^2\right)}}{3} - \frac{Br^3\sqrt{Ar}\sqrt{r_p\left(A + Br_p^2\right)}}{7A} + \frac{B^2r^5\sqrt{Ar}\sqrt{r_p\left(A + Br_p^2\right)}}{44A^2} - \frac{Ar_pR_z}{2} - \frac{Br_p^3R_z}{2} - \frac{AR_z^2}{4} - \frac{BR_z^4}{8} + \frac{2\sqrt{r_p\left(A + Br_p^2\right)}R_z\sqrt{AR_z}}{3}$$

$$+\frac{B\sqrt{r_p\left(A+Br_p^2\right)}R_z^3\sqrt{AR_z}}{7A}-\frac{B^2\sqrt{r_p\left(A+Br_p^2\right)}R_z^5\sqrt{AR_z}}{44A^2}. \tag{34}$$

where $A=-\frac{G_r}{A_1}+\frac{G_r\gamma R_z^2}{4A_1}-\frac{\sigma\rho\rho_e\varepsilon E_z}{A_1}-\frac{P}{A_1}$ and $B=-\frac{G_r\gamma}{8A_1}$. By evaluating $r=r_p$ into Eq. (34), the non-dimensional of velocity of fluid in the plug flow region yield

$$u(r_p)=\frac{Ar_p^2}{4}+\frac{Br_p^4}{8}+\frac{Ar_p^2}{2}+\frac{Br_p^4}{2}-\frac{2r_p\sqrt{Ar_p}\sqrt{r_p\left(A+Br_p^2\right)}}{3}-\frac{Br_p^3\sqrt{Ar_p}\sqrt{r_p\left(A+Br_p^2\right)}}{7A}$$
$$+\frac{B^2r_p^5\sqrt{Ar_p}\sqrt{r_p\left(A+Br_p^2\right)}}{44A^2}-\frac{Ar_pR_z}{2}-\frac{Br_p^3R_z}{2}-\frac{AR_z^2}{4}-\frac{BR_z^4}{8}+\frac{2\sqrt{r_p\left(A+Br_p^2\right)}R_z\sqrt{AR_z}}{3}$$
$$+\frac{B\sqrt{r_p\left(A+Br_p^2\right)}R_z^3\sqrt{AR_z}}{7A}-\frac{B^2\sqrt{r_p\left(A+Br_p^2\right)}R_z^5\sqrt{AR_z}}{44A^2}. \tag{35}$$

Substituting Eq. (20) into Eq. (12), the non-dimensional of mean velocity in Eq. (12) yield

$$u_m=\frac{2}{R_z^2}\left(\int_0^{r_p}u(r_p)rdr+\int_{r_p}^{R_z}u(r)rdr\right) \tag{36}$$

and Eq. (36) has been obtained by using integral method. It yields

$$u_m=\frac{2}{R_z^2}\Bigg[-\frac{B\sqrt{r_p\left(A+Br_p^2\right)}R_z^6}{22\sqrt{AR_z}}+\frac{B^2\sqrt{r_p\left(A+Br_p^2\right)}R_z^7\sqrt{AR_z}}{120A^2}+\frac{AR_z^3(4r_p+3R_z)}{48}+\frac{r_p}{2}\Bigg(-\frac{3Ar_p^2}{4}-\frac{5Br_p^4}{8}+$$
$$\frac{2r_p\sqrt{Ar_p}\sqrt{r_p(A+Br_p^2)}}{3}+\frac{Br_p^3\sqrt{Ar_p}\sqrt{r_p(A+Br_p^2)}}{7A}-\frac{B^2r_p^5\sqrt{Ar_p}\sqrt{r_p(A+Br_p^2)}}{44A^2}+\frac{Ar_pR_z}{2}+\frac{Br_p^3R_z}{2}+\frac{AR_z^2}{4}+\frac{BR_z^4}{8}-$$
$$\frac{2\sqrt{r_p\left(A+Br_p^2\right)}R_z\sqrt{AR_z}}{3}+R_z\sqrt{AR_z}-\frac{B\sqrt{r_p\left(A+Br_p^2\right)}R_z^3\sqrt{AR_z}}{7A}+\frac{B^2\sqrt{r_p\left(A+Br_p^2\right)}R_z^5\sqrt{AR_z}}{44A^2}+u_s\Bigg)+$$
$$\frac{R_z^2}{168}\Bigg[-24\sqrt{r_p\left(A+Br_p^2\right)}R_z\sqrt{AR_z}+7B\left(2r_p^3R_z+R_z^4\right)+84u_s\Bigg]+\frac{r_p^2}{18480A^2}\Bigg(385A^3\left[11r_p^2-12r_pR_z-\right.$$
$$\left.6R_z^2\right]-120AB\sqrt{r_p\left(A+Br_p^2\right)}\left[4r_p^3\sqrt{Ar_p}-11R_z^3\sqrt{AR_z}\right]+14B^2\sqrt{r_p\left(A+Br_p^2\right)}\left(4r_p^5\sqrt{Ar_p}-\right.$$
$$\left.15R_z^5\sqrt{AR_z}\right)-55A^2\Bigg[21B\left(-3r_p^4+4r_p^3R_z+R_z^4\right)+8\Bigg(8r_p\sqrt{Ar_p}\sqrt{r_p\left(A+Br_p^2\right)}-$$
$$\left.14\sqrt{r_p\left(A+Br_p^2\right)}R_z\sqrt{AR_z}+21u_s\Bigg)\Bigg]\Bigg)\Bigg] \tag{37}$$

By applying Eq. (20) into Eq. (14), it is simplified as follows

$$\frac{\partial C}{\partial t}+u\frac{\partial C}{\partial z^*}=\left(\ell^2+\frac{1}{Pe^2}\frac{\partial^2}{\partial z^{*2}}\right)C, \tag{38}$$

where

$$Pe = \frac{R_0 u_0}{D_m}. \tag{39}$$

The Peclet number, Pe for the flow in a circular pipe is provided by Dash *et al.,* [21]. The method proposed by Gill and Sankarasubramanian [16] is used, and the solution of Eq. (38) is assumed to be a derivative series expansion involving $\partial^i C_m / \partial z_z^i$. The following is the demonstration

$$C(r,z,t) = C_m(z_1,t) + \sum_{i=1}^{\infty} f_i(r,t) \frac{\partial^i C_m(z_1,t)}{\partial z_1^i}, \tag{40}$$

where C_m and $f_i(r,t)$ are the mean concentration of the solute over a cross-sectional area of the geometry, is the dispersion function associated with $\partial^i C_m / \partial z_z^i$. By substituting Eq. (20) into Eq. (16) – (19), the non-dimensional of initial and boundary conditions of convective-diffusion equation are obtained as

$$C(r,z,0) = \begin{cases} 1 \text{ if } |z| \le \frac{z_s}{2}, \\ 0 \text{ if } |z| > \frac{z_s}{2}, \end{cases} \tag{41}$$

$$C(r,\infty,t) = 0, \tag{42}$$

$$\frac{\partial C}{\partial r}(0,z,t) = 0, \tag{43}$$

and

$$\frac{\partial C}{\partial r}(R(z),z,t) = 0. \tag{44}$$

GDM is a derivative series expansion the approach of Gill and Sankarasubramanian [16] which given as

$$\frac{\partial C_m}{\partial t}(z_1,t) = \sum_{i=1}^{\infty} K_i(t) \frac{\partial^i C_m}{\partial z_z^i}(z_1,t). \tag{45}$$

where $K_i(t)$ is the transport coefficient given by

$$K_i(t) = \frac{\delta_{i2}}{\partial t} + 2\frac{\partial f_i}{\partial r}(1,t) - 2\int_0^{R(z)} f_{i-1}(r,t)u(r)rdr, i = 1,2,3,\ldots. \tag{46}$$

The effective axial diffusivity. δ_{ij} is given by

$$\delta_{ij} = \begin{cases} 0 \text{ if } i \neq j, \\ 1 \text{ if } i = j. \end{cases} \tag{47}$$

Using the initial condition Eq. (41) into Eq. (45), it yields $f_0(r,0) = 1$. Multiplying the solution in Eq. (45) with r and integrating it from 0 to $R(z)$ with the respect to r, it yields

$$C_m(z_1,t) = 2\int_0^{R(z)} C(r,z_1,t)rdr. \tag{48}$$

In calculating the mean concentration, $C_m(z_1,t)$, the dispersion function of $f_1(r,t)$ plays an important role Thus, the dispersion function is shown as follows

$$f_1(r,t) = f_{1s}(r) + f_{1t}(r,t), \tag{49}$$

where $f_{1s}(r)$ and $f_{1t}(r,t)$ are the dispersion functions in the steady and unsteady state that describes the time dependent nature of the dispersion of the solute. Therefore, the dispersion function at steady state is given by

$$\frac{1}{r}\frac{\partial}{\partial r}\left(r\frac{\partial f_{1s}}{\partial r}\right) - \left(u(r_p) - u_m\right) = 0 \text{ if } 0 \le r \le r_p \tag{50}$$

and the dispersion function in outer region is given as follows

$$\frac{1}{r}\frac{\partial}{\partial r}\left(r\frac{\partial f_{1s}}{\partial r}\right) - (u(r) - u_m) = 0 \text{ if } r_p \le r \le R(z). \tag{51}$$

Eq. (50) and Eq. (51) are solved using Eq. (50) to get f_{1s_-} and f_{1s_+}

$$\frac{df_{1s}}{dt}(0) = 0. \tag{52}$$

and

$$\frac{df_{1s}}{dr}R(z) = 0. \tag{53}$$

The steady dispersion function in the plug flow region, f_{1s_-} and outer flow region, f_{1s_+}. Thus, it yields

$$f_{1s_-} = CI - \frac{3Ar_p^4}{16} - \frac{5Br_p^6}{32} + \frac{r_p^3\sqrt{Ar_p}\sqrt{r_p(A+Br_p^2)}}{6} + \frac{Br_p^5\sqrt{Ar_p}\sqrt{r_p(A+Br_p^2)}}{28A} - \frac{B^2r_p^7\sqrt{Ar_p}\sqrt{r_p(A+Br_p^2)}}{176A^2} + \frac{Ar_p^3R_z}{12} + \frac{Br_p^5R_z}{12} + \frac{Br_p^2R_z^2}{32} + \frac{Br_p^2R_z^4}{96} - \frac{2r_p^2\sqrt{r_p(A+Br_p^2)}R_z\sqrt{AR_z}}{21} - \frac{Br_p^2\sqrt{r_p(A+Br_p^2)}R_z^3\sqrt{AR_z}}{77A} + \frac{B^2r_p^2\sqrt{r_p(A+Br_p^2)}R_z^5\sqrt{AR_z}}{660A^2} \tag{54}$$

and

$$f_{1s_+} = CI - \frac{Ar^4}{64} - \frac{Br^6}{288} - \frac{Br^3r_p^3}{18} - \frac{67Ar_p^4}{576} - \frac{7Br_p^6}{72} + \frac{8r^3\sqrt{Ar_p}\sqrt{r_p(A+Br_p^2)}}{147} + \frac{4Br^5\sqrt{Ar_p}\sqrt{r_p(A+Br_p^2)}}{847A} - \frac{B^2r^7\sqrt{Ar_p}\sqrt{r_p(A+Br_p^2)}}{2475A^2} + \frac{11r_p^3\sqrt{Ar_p}\sqrt{r_p(A+Br_p^2)}}{98} + \frac{15Br_p^5\sqrt{Ar_p}\sqrt{r_p(A+Br_p^2)}}{484A} - \frac{19B^2r_p^7\sqrt{Ar_p}\sqrt{r_p(A+Br_p^2)}}{3600A^2} + \frac{Ar^2r_pR_z}{12} + \frac{Br^2r_p^3R_z}{12} + \frac{Ar^2R_z^2}{32} + \frac{Br^2R_z^4}{96} - \frac{2r^2\sqrt{r_p(A+Br_p^2)}R_z\sqrt{AR_z}}{21} - \frac{Br^2\sqrt{r_p(A+Br_p^2)}R_z^3\sqrt{AR_z}}{77A} + \frac{B^2r^2\sqrt{r_p(A+Br_p^2)}R_z^5\sqrt{AR_z}}{660A^2}, \tag{55}$$

where

$$CI = \frac{67Ar_p^4}{576} + \frac{7Br_p^6}{72} - \frac{11r_p^3\sqrt{Ar_p}\sqrt{r_p(A+Br_p^2)}}{98} - \frac{15Br_p^5\sqrt{Ar_p}\sqrt{r_p(A+Br_p^2)}}{484A} + \frac{19B^2r_p^7\sqrt{Ar_p}\sqrt{r_p(A+Br_p^2)}}{3600A^2} - \frac{Ar_p^6}{20R_z^2} - \frac{27Br_p^8}{640R_z^2} + \frac{15r_p^5\sqrt{Ar_p}\sqrt{r_p(A+Br_p^2)}}{484A} + \frac{19B^2r_p^7\sqrt{Ar_p}\sqrt{r_p(A+Br_p^2)}}{1320AR_z^2} - \frac{23B^2r_p^9\sqrt{Ar_p}\sqrt{r_p(A+Br_p^2)}}{9120A^2R_z^2} - \frac{7Ar_pR_z^3}{360} - \frac{7Br_p^3R_z^3}{360} - \frac{AR_z^4}{96} - \frac{5BR_z^6}{1152} + \frac{15\sqrt{r_p(A+Br_p^2)}R_z^3\sqrt{AR_z}}{539} + \frac{19B\sqrt{r_p(A+Br_p^2)}R_z^5\sqrt{AR_z}}{3630A} - \frac{23B\sqrt{r_p(A+Br_p^2)}R_z^7\sqrt{AR_z}}{34200A^2}. \quad (56)$$

The general solution of $f_{1t}(r,t)$ is given as

$$f_{1t}(r,t) = \sum_{m=1}^{\infty} A_m e^{-\lambda_m^2 t} J_0(\lambda_m r), \quad (57)$$

where

$$A_m = -\frac{2}{J_0^2(\lambda_m)} \int_0^{R(z)} J_0(\lambda_m r) f_{1s}(r) r dr. \quad (58)$$

Due to the complexity of the expressions involved, the dispersion function is not explicitly detailed here due to its very large expressions. Therefore, the complete mathematical expression for the dispersion function has not been included in the manuscript.

3. Results

This study examined the impact of temperature and electric field in Casson blood flow on the solute dispersion in blood as it flows through a stenosed artery, using GDM for analysis. By including temperature and electric field measurements into the research, a more comprehensive comprehension of the advancements in treatment for medical conditions may be achieved. The effect of temperature and electric field on velocity, u, function of steady dispersion, f_{1s}, function of unsteady dispersion, f_{1t} and function of dispersion, f_1 which is the combination of steady and unsteady dispersion functions have been analyzed. These analyzes helps researchers, engineers, and mathematicians improve mathematical methods in the biomedical sciences and improve modeling methodologies. A visual comparison between present result with Dash *et al.,* [21] has been shown for validation with previous study. This rigorous validation procedure not only confirms the accuracy of mathematical model but also highlights the applicable it is to actual biomedical situations. The fluid's impact on the solute dispersion mechanism has been further examined in the mean absorption, γ, electric field, E_z and height of stenosis, a.

3.1 Velocity

This section presents graphical computations of the impact of mean absorption, γ, electric field, E_z and height of stenosis, a. Upon solving the equation of momentum and determining the yield stress, the velocity data is acquired and interpreted by manipulating various components within the flow analytical expression.

Figure 2 illustrates the relationship between Casson fluid velocity, temperature, and electric field, as confirmed by Dash *et al.,* [21]. Apart from temperature and electric field influences, previous research demonstrates favorable Casson fluid velocity outcomes. The velocity observed in this investigation is consistent with the velocity reported in Dash *et al.,* [21]. This study assumes $\gamma = 0, E_z = 0$ and $a = 0$ with Grashof number $G_r = 1$ and stenosis radius, $R(z) = 1$. The validated

Casson fluid velocity's implications are significant in bioengineering and biomedical engineering, especially in enhancing microfluidic device precision for drug delivery and lab-on-a-chip systems. Controlling temperature and electric fields improves drug delivery accuracy, advancing biomedical applications.

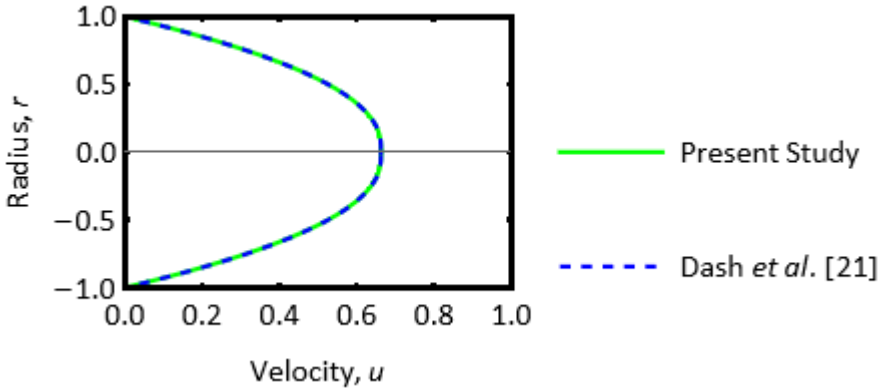

Fig. 2. Validation between the velocity of the Casson fluid and its temperature and electric field

Figure 3 depicts the fluctuations in velocity, u differencing in blood flow with different mean absorption, γ for $\mathrm{dp/dz} = -4, \mathrm{a} = 0.02, \mathrm{G_r} = 1, \mathrm{z} = 0.5, \mathrm{b} = 0, \mathrm{u_s} = 0, \mathrm{r_p} = 0.01, \sigma = 1, \quad \rho = 1, \rho_e = 1, \mathrm{E_z} = 1$,and $A_1 = 1$ for different mean absorption, $\gamma = 0, 0.2, 0.4, 0.6, 0.8$. Changes in mean absorption impact blood flow velocity, where higher mean absorption levels correspond to reduced temperature and increased velocity. An increase in mean absorption in arterial blood flow signifies greater energy absorption by the blood, potentially attributed to heightened metabolic activity or absorption from surrounding tissues. This elevated energy absorption reduces the available resources for maintaining blood temperature, leading to a decrease in temperature as a result.

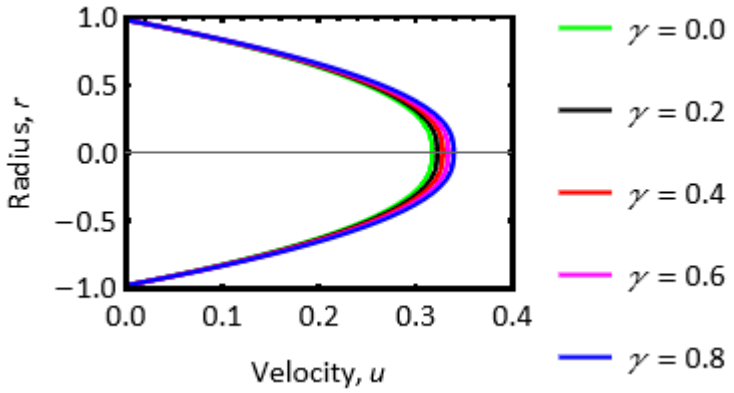

Fig. 3. The fluctuations in velocity, $\boldsymbol{u}$ differencing in blood flow with different mean absorption, $\boldsymbol{\gamma}$ for $\mathbf{dp/dz} = -\mathbf{4}, \mathbf{a} = \mathbf{0.02}, \mathbf{G_r} = \mathbf{1}, \mathbf{z} = \mathbf{0.5}, \mathbf{b} = \mathbf{0}, \mathbf{u_s} = \mathbf{0}, \mathbf{r_p} = \mathbf{0.01}, \boldsymbol{\sigma} = \mathbf{1}, \boldsymbol{\rho} = \mathbf{1}, \boldsymbol{\rho_e} = \mathbf{1}, \mathbf{E_z} = \mathbf{1}$,and $\boldsymbol{A_1} = \mathbf{1}$

Figure 4 depicts the variations of velocity, u for different values of electric field, E_z in the blood flow with $dp/dz = -4, a = 0.02, G_r = 1, z = 0.5, b = 0, u_s = 0, r_p = 0.01, \sigma = 1, \rho = 1, \rho_e = 1, \gamma = 1$, and $A_1 = 1$ for different mean absorption, $E_z = 0, 0.2, 0.4, 0.6, 0.8$. As the electric field increases, the velocity decreases. The electric field's impact on blood flow velocity in arteries depends

on various factors, including the field's characteristics and blood properties. Electrokinetic forces, like electrophoresis and electroosmosis, induced by the field, can influence charged particle movement in blood. This movement may alter the flow velocity profile, potentially leading to velocity decreases with stronger electric fields.

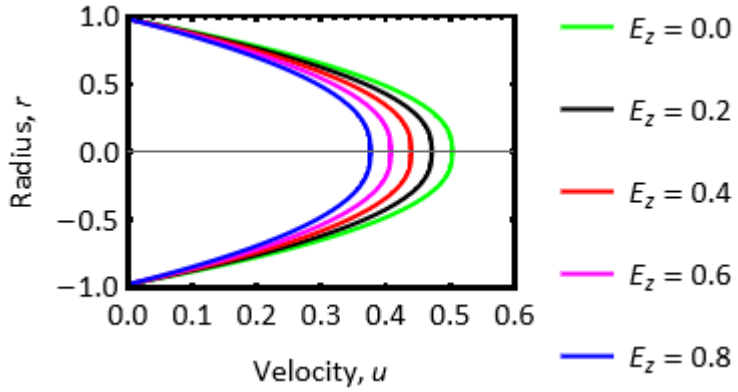

Fig. 4. The variations of velocity, $\boldsymbol{u}$ for different values of electric field, $\boldsymbol{E_z}$ in the blood flow with $\boldsymbol{dp/dz = -4, a = 0.02, G_r = 1, z = 0.5, b = 0, u_s = 0, r_p = 0.01, \sigma = 1, \rho = 1, \rho_e = 1, \gamma = 1}$, and $\boldsymbol{A_1 = 1}$

In conclusion, the ability to manipulate the velocity of Casson fluid through temperature and electric field adjustments has significant potential in advancing bioengineering and biomedical applications. It allows for more precise and effective medical device designs and treatment methods, ultimately improving patient care and treatment outcomes.

3.2 Steady Dispersion Function

Figure 5 depicts the validation between the steady dispersion function of the Casson fluid and its temperature and electric field, this outcome has been verified by Dash *et al.,* [21]. The outcome of the Casson fluid, disregarding the influence of temperature and electric field, demonstrates a favorable outcome in terms of the steady dispersion function of the Casson fluid as shown in the previous research. The steady dispersion function observed in this investigation is consistent with the steady dispersion function reported in Dash *et al.,* [21] in relation to temperature and electric field. In this research, when the mean absorption coefficient, electric field and height of stenosis have not been determined $(\gamma = 0, E_z = 0, a = 0)$, the Grashof number, G_r and radius of stenosis, $R(z)$ are denoted as $G_r = 1$ and $R(z) = 1$, respectively.

Figure 6 depicts the variations of steady dispersion function, f_{1s} for different mean absorption, γ for $\mathrm{dp/dz} = -4, \mathrm{a} = 0.02, \mathrm{G_r} = 1, \mathrm{z} = 0.5, \mathrm{b} = 0, \mathrm{r_p} = 0.01, \sigma = 1, \rho = 1, \rho_\mathrm{e} = 1, \mathrm{E_z} = 1,$ and $A_1 = 1$ for different mean absorption, $\gamma = 0, 0.2, 0.4, 0.6, 0.8$. In this case, the mean absorption affects the body temperature and hinders the dispersion function, resulting in a reduction in the dispersion function. As the temperature lowers towards the center of the artery, there is a simultaneous rise in the steady dispersion at the outside area near the wall.

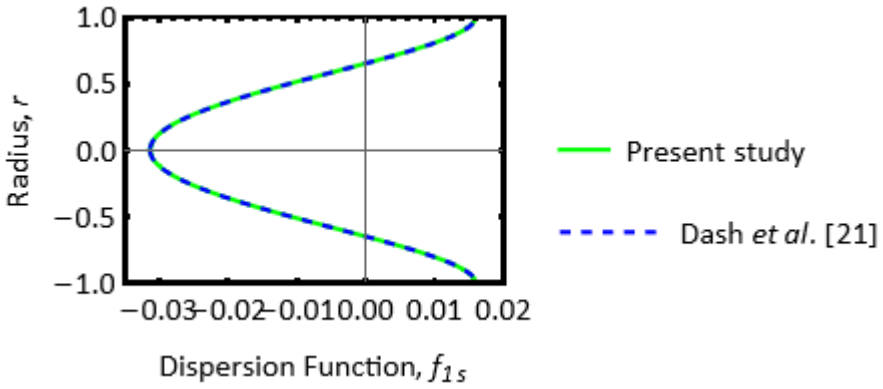

Fig. 5. The validation between the steady dispersion function

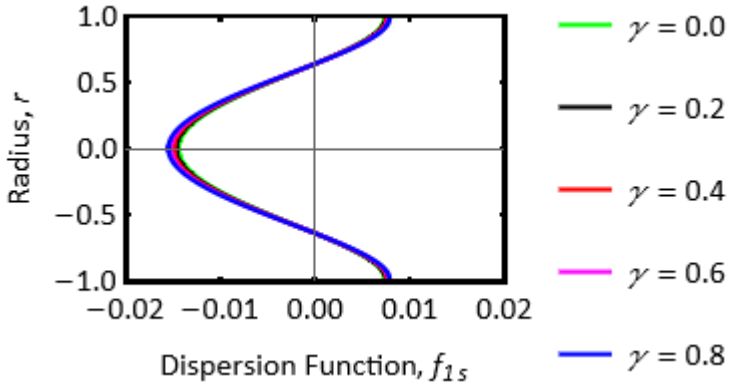

Fig. 6. The variations of steady dispersion function, $\boldsymbol{f_{1s}}$ for different mean absorption, $\boldsymbol{\gamma}$ for $\mathbf{dp/dz = -4, a = 0.02, G_r = 1, z = 0.5, b = 0, r_p = 0.01, \sigma = 1, \rho = 1, \rho_e = 1, E_z = 1}$, and $\boldsymbol{A_1 = 1}$

Figure 7 depicts the variations of steady dispersion function, f_{1s} for different values of electric field, E_z in the blood flow with $dp/dz = -4, a = 0.02, G_r = 1, z = 0.5, b = 0, r_p = 0.01, \sigma = 1, \rho = 1, \rho_e = 1, \gamma = 1$, and $A_1 = 1$ for different mean absorption, $E_z = 0, 0.2, 0.4, 0.6, 0.8$. When electric field increases, the steady dispersion function decreases. However, in this case, the height of the stenosis influences the dispersion function, resulting in a decrease. Conversely, electrical effects in vascular stenosis cause the dispersion function to steadily increase. This is significant because enhanced dispersion near the artery wall facilitates faster and more effective migration of solutes, suggesting the importance of reducing dispersion in the center while increasing it near the wall for improved medical outcomes.

In conclusion, the implications of steady dispersion function influenced by temperature and electric field are significant in bioengineering and biomedical engineering, particularly in medical device design and treatment strategies. Understanding the way dispersion function behaves under different conditions enhances the precision of biomedical device design reliant on accurate dispersion dynamics. This knowledge is critical for optimizing drug delivery systems, where temperature control and electric fields can effectively target therapeutic agents within the body, enhancing treatment efficacy and minimizing side effects.

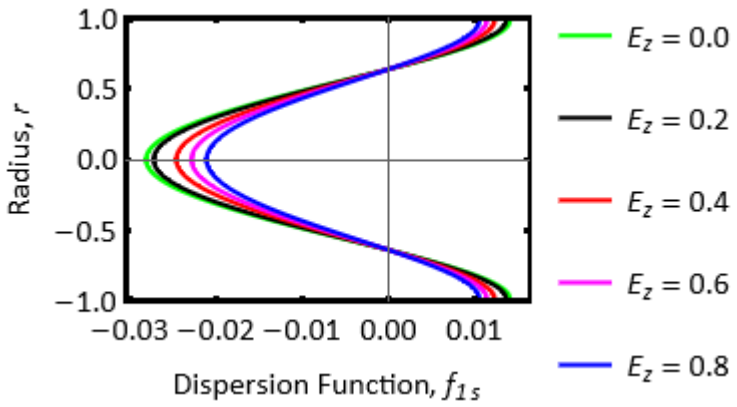

Fig. 7. The variations of steady dispersion function, $\boldsymbol{f_{1s}}$ for different values of electric field, $\boldsymbol{E_z}$ in the blood flow with $\boldsymbol{dp/dz = -4, a = 0.02, G_r = 1, z = 0.5, b = 0, r_p = 0.01, \sigma = 1, \rho = 1, \rho_e = 1, \gamma = 1}$, and $\boldsymbol{A_1 = 1}$

3.3 Unsteady Dispersion Function

Figure 8 depicts the validation between the unsteady dispersion function of the Casson fluid and its temperature and electric field, this outcome has been verified by Dash *et al.,* [21]. The outcome of the Casson fluid, disregarding the influence of temperature and electric field, demonstrates a favorable outcome in terms of the unsteady dispersion function of the Casson fluid as shown in the previous research. The unsteady dispersion function observed in this investigation is consistent with the unsteady dispersion function reported in Dash *et al.,* [21] in relation to temperature and electric field. In this research, when the mean absorption coefficient, electric field and height of stenosis have not been determined $(\gamma = 0, E_z = 0, a = 0)$, the Grashof number, G_r and radius of stenosis, $R(z)$ are denoted as $G_r = 1$ and $R(z) = 1$, respectively.

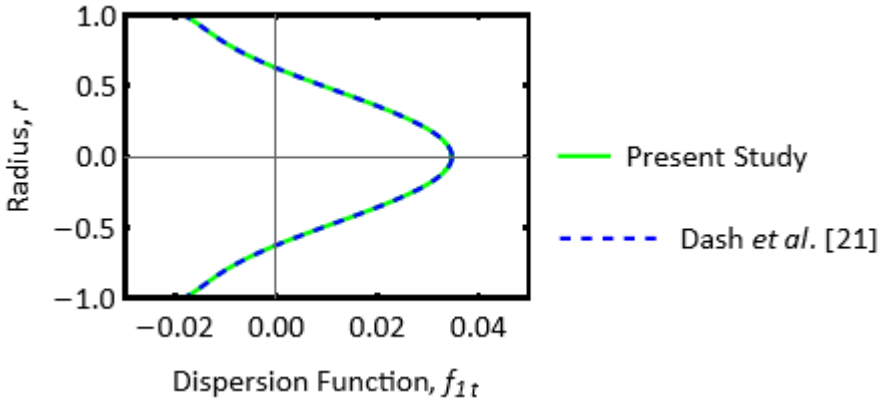

Fig. 8. The validation between the unsteady dispersion function

Figure 9 depicts the variations of unsteady dispersion function, f_{1t} for different values of mean absorption, γ for $dp/dz = -4, a = 0.02, G_r = 1, z = 0.5, t = 0.1, b = 0, r_p = 0.01, \sigma = 1, \rho = 1, \rho_e = 1, E_z = 1$, and $A_1 = 1$ for different mean absorption, $\gamma = 0, 0.2, 0.4, 0.6, 0.8$. In this case, the mean absorption affects the body temperature and disrupts the dispersion function, resulting in an increase in dispersion function. The heat transfer factor has a considerable impact on the longitudinal propagation in the flow through tubes with walls that are moderately or minimally reactive. Tiwari *et al.,* [19] stated that the transportation of nutrients to physiological systems or the administration

of medications to tissues during medical treatments requiring elevated temperatures might be somewhat impaired, resulting in potential delays, owing to the slightly elevated temperatures caused by certain medical procedures.

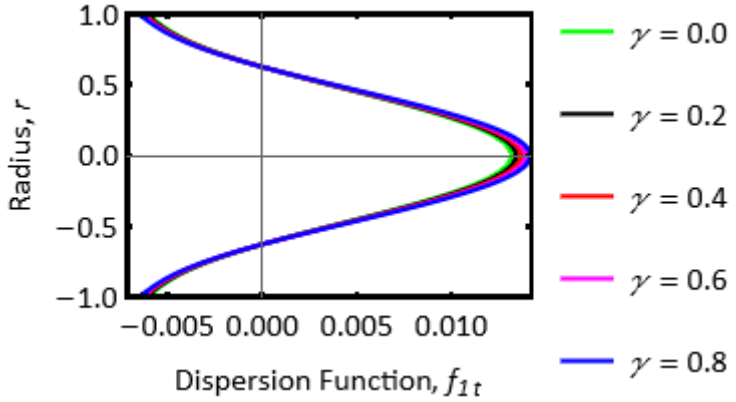

Fig. 9. The variations of unsteady dispersion function, $\boldsymbol{f_{1t}}$ for different values of mean absorption, $\boldsymbol{\gamma}$ for $\boldsymbol{dp/dz = -4, a = 0.02, G_r = 1, z = 0.5, t = 0.1, b = 0,\ r_p = 0.01, \sigma = 1, \rho = 1, \rho_e = 1, E_z = 1}$, and $\boldsymbol{A_1 = 1}$

Figure 10 depicts the variations of unsteady dispersion function, f_{1t} for different values of electric field, E_z in the blood flow with $dp/dz = -4, a = 0.02, t = 0.1, G_r = 1, z = 0.5, b = 0, r_p = 0.01, \sigma = 1, \rho = 1, \rho_e = 1, \gamma = 1,$ and $A_1 = 1$ for different mean absorption, $E_z = 0, 0.2, 0.4, 0.6, 0.8$. When electric field inclined, the unsteady dispersion function inclined. As time progresses, there is a decrease in the unsteady dispersion function. At the initial time (time zero), the unsteady dispersion function reaches its peak. However, as time elapses, the unsteady dispersion function gradually diminishes, approaching zero.

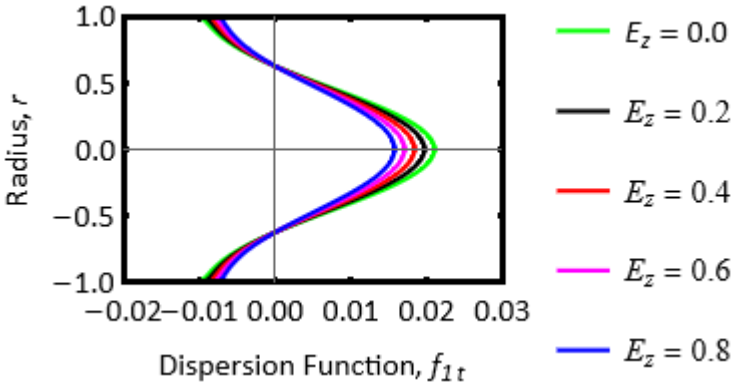

Fig. 10. The variations of unsteady dispersion function, $\boldsymbol{f_{1t}}$ for different values of electric field, $\boldsymbol{E_z}$ in the blood flow with $\boldsymbol{dp/dz = -4, a = 0.02, t = 0.1, G_r = 1, z = 0.5, b = 0, r_p = 0.01, \sigma = 1, \rho = 1, \rho_e = 1, \gamma = 1}$, and $\boldsymbol{A_1 = 1}$

In conclusion, in bioengineering, the ability to control unsteady dispersion function opens avenues for developing advanced diagnostic tools and therapeutic approaches that respond dynamically to physiological changes. For instance, microfluidic devices can be designed to adapt and optimize dispersion patterns in real-time, enhancing their utility in personalized medicine and point-of-care diagnostics. Moreover, in medical device design, understanding and harnessing unsteady

dispersion can ensure the reliability and effectiveness of devices used for continuous monitoring and precise delivery of treatments. Thus, integrating the understanding of unsteady dispersion function under temperature and electric field influences promises significant advancements in bioengineering and biomedical applications. It empowers the development of more responsive and effective medical devices and treatment strategies tailored to individual patient needs, ultimately enhancing healthcare outcomes and patient well-being.

3.4 Dispersion Function

Figure 11 depicts the validation between the dispersion function of the Casson fluid and its temperature and electric field, this outcome has been verified by Dash *et al.,* [21]. The outcome of the Casson fluid, disregarding the influence of temperature and electric field, demonstrates a favorable outcome in terms of the dispersion function of the Casson fluid as shown in the previous research. The dispersion function observed in this investigation is consistent with the dispersion function reported in Dash *et al.,* [21] in relation to temperature and electric field. In this research, when the mean absorption coefficient, electric field and height of stenosis have not been determined $(\gamma = 0, E_z = 0, a = 0)$, the Grashof number, G_r and radius of stenosis, $R(z)$ are denoted as $G_r = 1$ and $R(z) = 1$, respectively.

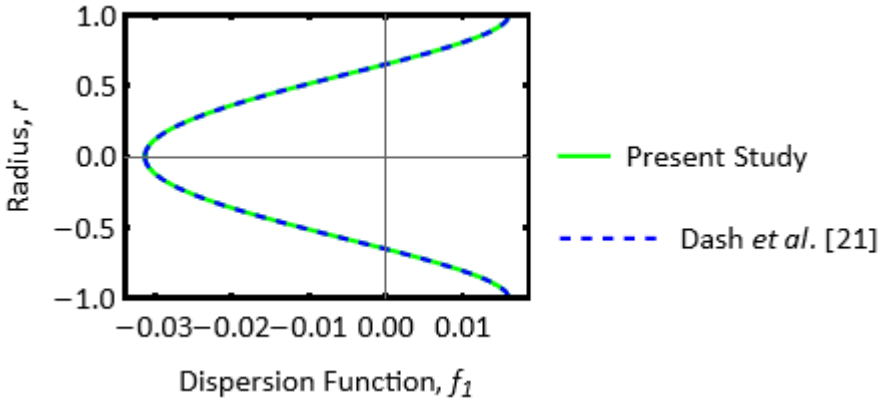

Fig. 11. The validation between the dispersion function

Figure 12 depicts the variations of dispersion function, f_1 for different values of mean absorption, γ for $dp/dz = -4, a = 0.02, G_r = 1, z = 0.5, b = 0, r_p = 0.01, \sigma = 1, \rho = 1, \rho_e = 1, t = 0.1, E_z = 1$, and $A_1 = 1$ for different mean absorption, $\gamma = 0, 0.2, 0.4, 0.6, 0.8$. As the mean absorption value increases, the dispersion function tends to decrease. As mean absorption rises in blood flow within an artery, the dispersion function decreases due to heightened substance uptake, resulting in reduced dispersion. This elevated absorption facilitates more efficient removal of substances from the bloodstream, thereby decreasing their dispersion and ultimately lowering the dispersion function.

Figure 13 depicts the variations of dispersion function, f_1 for different values of electric field, E_z in the blood flow with $dp/dz = -4, a = 0.02, G_r = 1, z = 0.5, b = 0, t = 0.1, r_p = 0.01, \sigma = 1, \rho = 1, \rho_e = 1, \gamma = 1$, and $A_1 = 1$ for different mean absorption, $E_z = 0, 0.2, 0.4, 0.6, 0.8$. When electric field increases, the dispersion function decreases. An increase in the electric field leads to stronger forces exerted on charged particles within the flow. This enhances electrophoretic motion, causing charged particles to migrate towards specific regions rather than dispersing throughout the flow. Consequently, this concentration of particles reduces dispersion function.

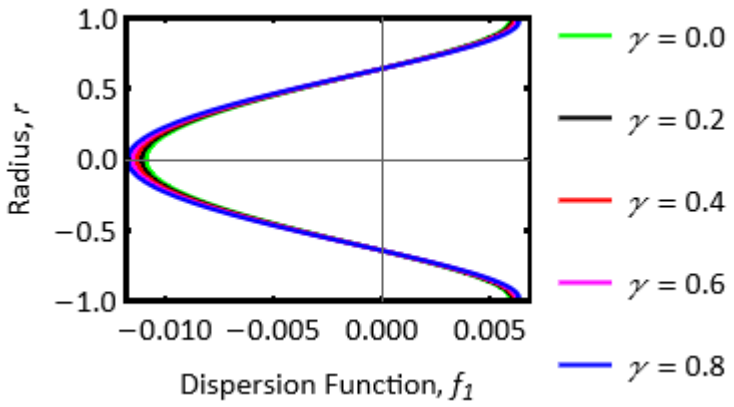

Fig. 12. The variations of dispersion function, $\boldsymbol{f_1}$ for different values of mean absorption, $\boldsymbol{\gamma}$ for $\boldsymbol{dp/dz = -4, a = 0.02, G_r = 1, z = 0.5, b = 0, r_p = 0.01, \sigma = 1, \rho = 1, \rho_e = 1, t = 0.1, E_z = 1}$, and $\boldsymbol{A_1 = 1}$

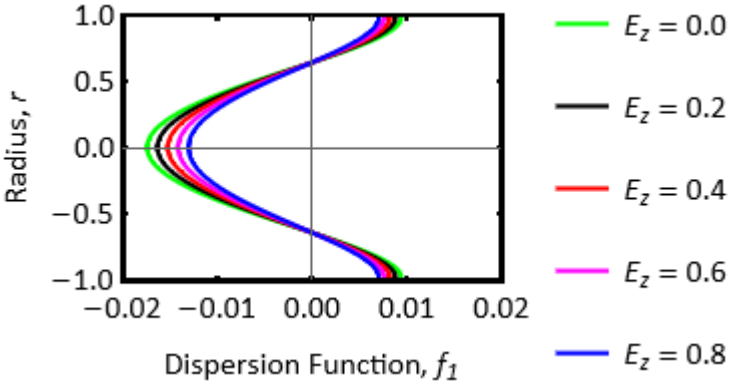

Fig. 13. The variations of dispersion function, $\boldsymbol{f_1}$ for different values of electric field, $\boldsymbol{E_z}$ in the blood flow with $\boldsymbol{dp/dz = -4, a = 0.02, G_r = 1, z = 0.5, b = 0, t = 0.1, r_p = 0.01, \sigma = 1, \rho = 1, \rho_e = 1, \gamma = 1}$, and $\boldsymbol{A_1 = 1}$

In conclusion, the modulation of dispersion function by temperature and electric field has significant implications in bioengineering and biomedical engineering, especially in the development of innovative medical devices and treatments. This understanding enables the creation of advanced diagnostic tools and therapeutic approaches that can adapt to biological conditions. For instance, microfluidic devices can be engineered to dynamically adjust dispersion patterns, enhancing accuracy in disease diagnostics and personalized treatment strategies. This knowledge also ensures the reliability and efficiency of medical devices used for continuous monitoring and precise drug delivery. Overall, leveraging dispersion function influenced by temperature and electric field promises to advance biomedical applications, leading to more effective healthcare solutions tailored to individual patient needs and improving overall treatment outcomes.

4. Conclusions

This work employs an innovative approach to examine the impact of temperature and electric field on the spread of solutes inside a stenosed artery in Casson blood flow. This approach is based on the physiological accuracy of the circulatory system and seeks to enhance our understanding of the process of mixing and the distribution of drugs to tissues via arterial blood vessels. An extensive

analysis has been conducted on the impact of temperature and electric field on velocity, as well as the steady and unsteady dispersion functions. It has been shown that these traits have a major impact on these amounts by providing new insights with important implications for biomedical engineering, fluid dynamics and medical pyhsics. The uniqueness and rigor of study's approach are demonstrated by the application of the binomial series expansion to difficult integration problems, which offers important resources to the academic community of mathematicians, biomedical engineers, fluid dynamicists, and medical researchers. The dispersion function has been determined using GDM, resulting in an analytical solution. The current research focuses on the following crucial determinations

i. Velocity and unsteady dispersion function increase with increasing mean absorption affecting the temperature. Under the prevalence of mean absorption, the duration for the diffusion process to finalize is notably reduced.
ii. Steady dispersion function and overall dispersion function decrease with increasing mean absorption affecting the temperature. Casson fluid starts to reduce with the increase in mean absorption, which further decreases the dispersion function after a certain value.
iii. Velocity decreases with increasing electric field. The dominance of the electric field inclines the peak of blood velocity.
iv. Steady dispersion function and overall dispersion function increase with increasing electric field. The study takes into account the electric field, where solute dispersion exhibits varying behavior based on the value of this parameter.
v. Unsteady dispersion function decreases with increasing electric field. The dispersion function falls as a result of insufficient solute particles diffusing effectively over the length of the artery.

Therefore, this research on solute dispersion in Casson blood flow through stenosed arteries, influenced by temperature and electric fields, represents a significant advancement in understanding physiological fluid dynamics and its implications for biomedical applications. By meticulously analyzing velocity and dispersion functions under varying conditions, the study not only enhances theoretical models in fluid dynamics but also provides practical insights crucial for optimizing drug delivery strategies in cardiovascular medicine. The innovative use of binomial series expansions to tackle complex integration challenges underscores the methodological rigor of the study, offering valuable tools for mathematicians and engineers involved in biomedical research. These findings not only contribute to advancing medical physics but also hold promise for guiding the development of more effective medical devices. Future research directions focusing on the impact of catheter radius and stenosis size on blood flow within stenosed arteries will further enrich our understanding and facilitate more targeted therapeutic interventions in cardiovascular care.

Acknowledgement
This research was not funded by any grant.

References

[1] Cleveland Clinic. "Cardiovascular System." September, 9, 2021.
[2] Mayo Clinic Staff. "Arteriosclerosis / atherosclerosis." Mayo Clinic, July 1, 2022.
[3] Sun, Mingzhuang, Shaoning Zhu, Yihao Wang, Yawei Zhao, Kaixin Yan, Xiaolong Li, Xueting Wang et al. "Effect of inflammation on association between cancer and coronary artery disease." *BMC Cardiovascular Disorders* 24, no. 1 (2024): 72. https://doi.org/10.1186/s12872-023-03613-0
[4] Toghraie, Davood, Navid Nasajpour Esfahani, Majid Zarringhalam, Nima Shirani, and Sara Rostami. "Blood flow analysis inside different arteries using non-Newtonian Sisko model for application in biomedical engineering."

Computer methods and programs in biomedicine 190 (2020): 105338. https://doi.org/10.1016/j.cmpb.2020.105338

[5] Ponalagusamy, R., and D. Murugan. "Transport of a reactive solute in electroosmotic pulsatile flow of non-Newtonian fluid through a circular conduit." *Chinese Journal of Physics* 81 (2023): 243-269. https://doi.org/10.1016/j.cjph.2022.11.002

[6] Chakraborty, Suman. "Electrokinetics with blood." *Electrophoresis* 40, no. 1 (2019): 180-189. https://doi.org/10.1002/elps.201800353

[7] Blair, GW Scott. "An equation for the flow of blood, plasma and serum through glass capillaries." *Nature* 183, no. 4661 (1959): 613-614. https://doi.org/10.1038/183613a0

[8] Casson, N. "Rheology of disperse systems." *Flow Equation for Pigment Oil Suspensions of the Printing Ink Type. Rheology of Disperse Systems* (1959): 84-102.

[9] Merrill, E. W., A. M. Benis, E. R. Gilliland, T. K. Sherwood, and E. W. Salzman. "Pressure-flow relations of human blood in hollow fibers at low flow rates." *Journal of Applied Physiology* 20, no. 5 (1965): 954-967. https://doi.org/10.1038/206617a0

[10] Murugan, D., Ashis Kumar Roy, R. Ponalagusamy, and O. Anwar Bég. "Tracer dispersion due to pulsatile casson fluid flow in a circular tube with chemical reaction modulated by externally applied electromagnetic fields." *International Journal of Applied and Computational Mathematics* 8, no. 5 (2022): 221. https://doi.org/10.1007/s40819-022-01412-3

[11] Noranuar, Wan Nura'in Nabilah, Ahmad Qushairi Mohamad, Lim Yeou Jiann, and Sharidan Shafie. "Analytical Simulation of Magnetohydrodynamics Casson Blood Flow using CNTs in a Channel with Atherosclerosis Condition." *Semarak Current Biomedical Technology Research Journal* 1, no. 1 (2024): 1-17.

[12] Azmi, Wan Faezah Wan, Ahmad Qushairi Mohamad, Lim Yeou Jiann, and Sharidan Shafie. "Porosity and Slip Velocity Effects on MHD Pulsatile Casson Fluid in a Cylinder." *Semarak International Journal of Nanotechnology* 1, no. 1 (2024): 13-28.

[13] Taylor, Geoffrey Ingram. "Dispersion of soluble matter in solvent flowing slowly through a tube." *Proceedings of the Royal Society of London. Series A. Mathematical and Physical Sciences* 219, no. 1137 (1953): 186-203. https://doi.org/10.1098/rspa.1953.0139

[14] Aris, Rutherford. "On the dispersion of a solute in a fluid flowing through a tube." *Proceedings of the Royal Society of London. Series A. Mathematical and Physical Sciences* 235, no. 1200 (1956): 67-77. https://doi.org/10.1098/rspa.1956.0065

[15] Gill, W. N., and R. Sankarasubramanian. "Exact analysis of unsteady convective diffusion." *Proceedings of the Royal Society of London. A. Mathematical and Physical Sciences* 316, no. 1526 (1970): 341-350.

[16] William N. Gill, and Sankarasubramanian, R. "Unsteady convective diffusion with interphase mass transfer." *Proceedings of the Royal Society of London. A. Mathematical and Physical Sciences* 333, no. 1592 (1973): 115-132. https://doi.org/10.1098/rspa.1973.0051

[17] Zaperi, Nur Husna Amierah Mohd, and Nurul Aini Jaafar. "Solute Dispersion in Casson Blood Flow through an Artery with the Effect of Electric Field." *Journal of Research in Nanoscience and Nanotechnology* 9, no. 1 (2023): 13-34. https://doi.org/10.37934/jrnn.9.1.1334

[18] Zaperi, Nur Husna Amierah Mohd, and Nurul Aini Jaafar. "Solute Dispersion in Casson Blood Flow through a Stenosed Artery with the Effect of Magnetic Field." *Semarak International Journal of Applied Sciences and Engineering Technology* 1, no. 1 (2024): 1-17.

[19] Tiwari, Ashish, Pallav Dhanendrakumar Shah, and Satyendra Singh Chauhan. "Unsteady solute dispersion in two-fluid flowing through narrow tubes: A temperature-dependent viscosity approach." *International Journal of Thermal Sciences* 161 (2021): 106651. https://doi.org/10.1016/j.ijthermalsci.2020.106651

[20] Verma, Narendra Kumar, Shailesh Mishra, Shafi Ullah Siddiqui, and Ram Saran Gupta. "Effect of slip velocity on blood flow through a catheterized artery." *Applied mathematics* 2, no. 6 (2011): 764. https://doi.org/10.4236/am.2011.26102

[21] Dash, R. K., G. Jayaraman, and K. N. Mehta. "Shear augmented dispersion of a solute in a Casson fluid flowing in a conduit." *Annals of Biomedical Engineering* 28 (2000): 373-385. https://doi.org/10.1114/1.287